

Metal-mediated DNA strand displacement and molecular device operations based on base-pair switching of 5-hydroxyuracil nucleobases

Received: 23 October 2022

Accepted: 13 July 2023

Published online: 24 August 2023

Check for updates

Yusuke Takezawa¹✉, Keita Mori¹, Wei-En Huang¹, Kotaro Nishiyama¹, Tong Xing¹, Takahiro Nakama¹ & Mitsuhiko Shionoya¹✉

Rational design of self-assembled DNA nanostructures has become one of the fastest-growing research areas in molecular science. Particular attention is focused on the development of dynamic DNA nanodevices whose configuration and function are regulated by specific chemical inputs. Herein, we demonstrate the concept of metal-mediated base-pair switching to induce inter- and intramolecular DNA strand displacement in a metal-responsive manner. The 5-hydroxyuracil (U^{OH}) nucleobase is employed as a metal-responsive unit, forming both a hydrogen-bonded $\text{U}^{\text{OH}}\text{-A}$ base pair and a metal-mediated $\text{U}^{\text{OH}}\text{-Gd}^{\text{III}}\text{-U}^{\text{OH}}$ base pair. Metal-mediated strand displacement reactions are demonstrated under isothermal conditions based on the base-pair switching between $\text{U}^{\text{OH}}\text{-A}$ and $\text{U}^{\text{OH}}\text{-Gd}^{\text{III}}\text{-U}^{\text{OH}}$. Furthermore, metal-responsive DNA tweezers and allosteric DNazymes are developed as typical models for DNA nanodevices simply by incorporating U^{OH} bases into the sequence. The metal-mediated base-pair switching will become a versatile strategy for constructing stimuli-responsive DNA nanostructures, expanding the scope of dynamic DNA nanotechnology.

Rational design of self-assembled DNA nanostructures, termed DNA nanotechnology^{1,2}, is one of the fastest-growing research areas in molecular science. Hybridization based on strict base-pairing rules has made DNA an excellent building block for constructing precisely defined molecular structures at the nanometer scale^{3,4}. Of particular interest is the development of dynamic DNA nanodevices whose configuration and function are regulated by specific chemical inputs⁵⁻⁷. Such complex DNA systems are usually manipulated by toehold-mediated DNA strand displacement reactions (SDRs)^{8,9}, which use DNA or RNA strands as input signals. There is also growing interest in the operation of DNA nanodevices by diverse signals such as pH¹⁰, light¹¹⁻¹³, and small molecules^{14,15}. Precise chemical modifications¹⁶ and conjugation with aptamers¹⁷ and antibodies¹⁸ have shown that

DNA molecules can respond to specific chemical inputs or environmental stimuli.

Metal ions are often employed as chemical inputs in supramolecular chemistry¹⁹. Over the past few decades, a variety of metal-responsive molecular switches and machines have been synthesized²⁰⁻²² by exploiting the specific affinity between ligands and metal species. However, the construction of metal-responsive DNA systems is still in its infancy, as it has relied on limited types of metal-DNA interactions, such as potassium-dependent induction of G-quadruplexes²³ and metal-mediated formation of interstrand T-Hg^{II}-T and C-Ag^I-C complexes²⁴ (termed as metal-mediated base pairs²⁵⁻²⁷).

In this study, we demonstrate the concept of metal-mediated base-pair switching to induce inter- and intramolecular strand exchange in

¹Department of Chemistry, Graduate School of Science, The University of Tokyo, 7-3-1 Hongo, Bunkyo-ku, Tokyo 113-0033, Japan.

✉ e-mail: takezawa@chem.s.u-tokyo.ac.jp; shionoya@chem.s.u-tokyo.ac.jp

response to metal ions (Fig. 1). First, metal-mediated regulation of SDRs, one of the most fundamental processes for operating DNA nanodevices and computing circuits, is examined. Metal-mediated manipulation of DNA tweezers²⁸ and regulation of the catalytic activity of a deoxyribozyme (DNAzyme)²⁹ are also studied as typical models of DNA molecular devices. To enable rational sequence design of metal-responsive DNA structures, we utilize a noncanonical bifacial nucleobase, 5-hydroxyuracil (U^{OH}), which can form both a Watson–Crick type hydrogen-bonded U^{OH} –A base pair and a metal-mediated U^{OH} –M– U^{OH} base pair (M = Gd^{III} , etc.) with its bidentate metal-binding site (i.e., an adjacent 4-carbonyl and a 5-hydroxy groups)^{30–32}. Our previous studies have shown that the thermal stability of DNA duplexes containing U^{OH} – U^{OH} mismatches is significantly enhanced by the formation of U^{OH} – Gd^{III} – U^{OH} base pairs, while duplexes with U^{OH} –A base pairs are destabilized by the addition of Gd^{III} . This raises the possibility that the base-pairing partner of the U^{OH} bases can be switched in response to Gd^{III} . We therefore conceived of the idea that Gd^{III} -mediated base-pair switching between U^{OH} –A and U^{OH} – Gd^{III} – U^{OH} can be applied to the construction of dynamic DNA systems such as SDRs, DNA tweezers, and allosteric DNAzymes. Since U^{OH} nucleobases can be easily synthesized and incorporated into DNA strands, sequence design strategies using metal-responsive U^{OH} bases are expected to greatly expand the toolbox of dynamic DNA nanotechnology.

Results

Metal-mediated DNA strand displacement reactions (SDRs)

Dynamic DNA nanotechnology relies heavily on SDRs^{8,9}. SDRs are usually initiated by the binding of an invading strand to a single-stranded segment called a toehold. The development of SDRs triggered by stimuli other than oligonucleotides is increasingly attracting attention as an expansion of the DNA nanotechnology toolbox. In the past, binding of small molecules to aptamers¹⁵, pH changes³³, photoirradiation^{34,35}, and metal–ligand interaction^{36,37} have been employed to trigger SDRs. In this study, we investigated toehold-free, metal-mediated SDRs based on base-pair switching between U^{OH} –A and U^{OH} – Gd^{III} – U^{OH} at the terminus of each strand.

Prior to the SDR experiments, metal-mediated regulation of DNA hybridization was first studied using oligonucleotides containing four U^{OH} bases. Three 16-mer DNA strands were designed so that strand 1 can hybridize with strand 2 via U^{OH} – Gd^{III} – U^{OH} base pairing and with

strand 3 via U^{OH} –A base pairing at their termini (Fig. 2a). The thermal stability of each duplex (i.e., 1-2 and 1-3) in the absence and presence of Gd^{III} ions was evaluated by melting analysis (Supplementary Figs. 1a and 2a). Under conditions without Gd^{III} ions, the melting temperature (T_m) of duplex 1-3 containing four U^{OH} –A pairs was higher ($T_m = 45.3^\circ\text{C}$) than that of duplex 1-2 containing four U^{OH} – U^{OH} mismatch pairs (37.9°C). Similar to previous studies^{30,31}, the addition of Gd^{III} ions significantly increased the stability of duplex 1-2 ($\Delta T_m = +26.2^\circ\text{C}$ with 4 equiv of Gd^{III} ions). The stabilization of the duplex by Gd^{III} was ascribed to the formation of interstrand U^{OH} – Gd^{III} – U^{OH} complexes, which was confirmed by UV titration experiments and ESI-TOF mass spectrometry (Supplementary Fig. 1). On the other hand, duplex 1-3 was destabilized by the addition of Gd^{III} ions ($\Delta T_m = -6.4^\circ\text{C}$). This may be due to the weakening of the U^{OH} –A base pairing by the binding of Gd^{III} ions to the U^{OH} bases^{30–32} (Supplementary Fig. 2). As a result, duplex 1-2 containing U^{OH} – Gd^{III} – U^{OH} base pairs was found to be much more stable than duplex 1-3 containing U^{OH} –A base pairs upon addition of Gd^{III} (Fig. 2b). These results indicate that the addition of Gd^{III} ions reversed the order of the stability of the duplexes. The same trend was observed for DNA strands containing three U^{OH} bases (Supplementary Fig. 3). Addition of Gd^{III} ions (3 equiv) stabilized duplex 1'-2' with three U^{OH} – U^{OH} pairs ($\Delta T_m = +25.2^\circ\text{C}$) and destabilized duplex 1'-3' with three U^{OH} –A pairs ($\Delta T_m = -4.4^\circ\text{C}$). The degree of duplex (de)stabilization (ΔT_m) was slightly greater when four U^{OH} bases were incorporated (Supplementary Fig. 4). Incorporation of more than four U^{OH} bases was thought to cause undesirable intramolecular metal complexation. Therefore, DNA strands 1 and 2 containing four consecutive U^{OH} bases were employed in the SDR experiments.

Next, an equimolar mixture of strands 1, 2, and 3 (labeled with a fluorophore FAM) was annealed in the absence and presence of Gd^{III} ions to see which duplex (1-2 or 1-3) is preferentially formed. Native polyacrylamide gel electrophoresis (PAGE) analysis confirmed products containing strand 3 by visualization with FAM fluorescence (Fig. 2c) and all products by further staining (Supplementary Fig. 5). The results revealed that duplex 1-3 was mainly formed (81%) under the Gd^{III} -free condition. The addition of Gd^{III} ions (4 equiv) resulted in the release of strand 3 (90%) and the formation of duplex 1-2. UV spectroscopy showed that hybridization of duplex 1-2 was accompanied by metal complexation of the U^{OH} bases (Fig. 2d). The yield of the formed duplex increased as the amount of Gd^{III} ions increased from 0 to 4.0

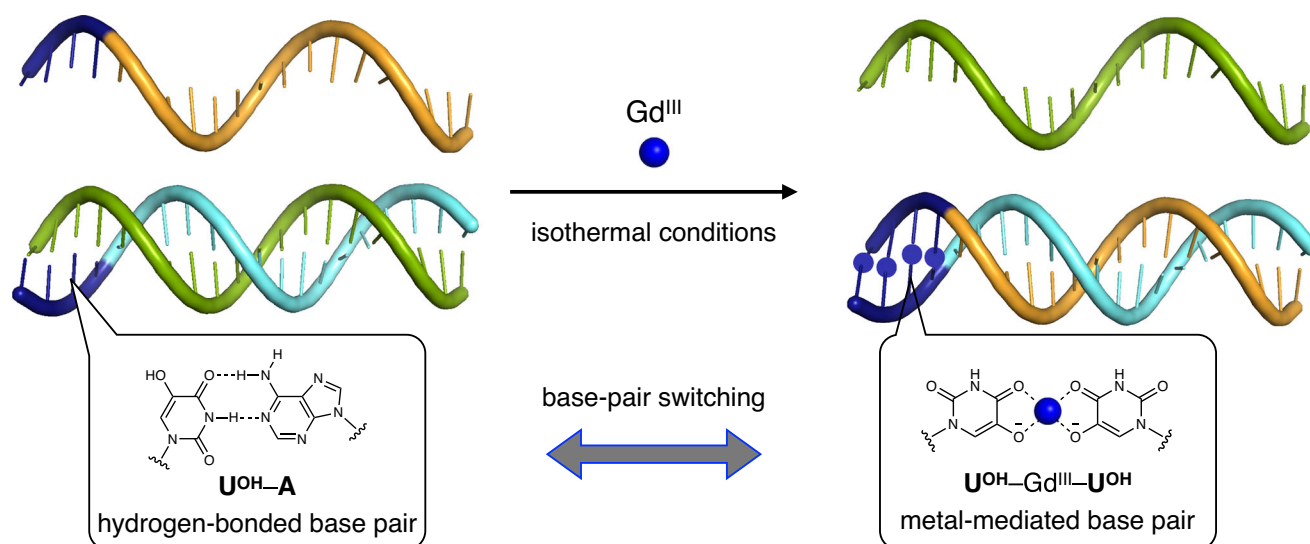


Fig. 1 | Schematic representation of metal-mediated DNA strand displacement reactions (SDRs) induced by base-pair switching of 5-hydroxyuracil (U^{OH}) nucleobases. Base-pair switching between hydrogen-bonded U^{OH} –A pairs and metal-mediated unnatural U^{OH} – Gd^{III} – U^{OH} pairs can induce SDRs in response to Gd^{III}

ions. U^{OH} nucleotides in the DNA strands are highlighted in navy blue. Other possible coordinating ligands on the Gd^{III} ions, such as water molecules and neighboring nucleobases, are not shown for simplicity³⁰.

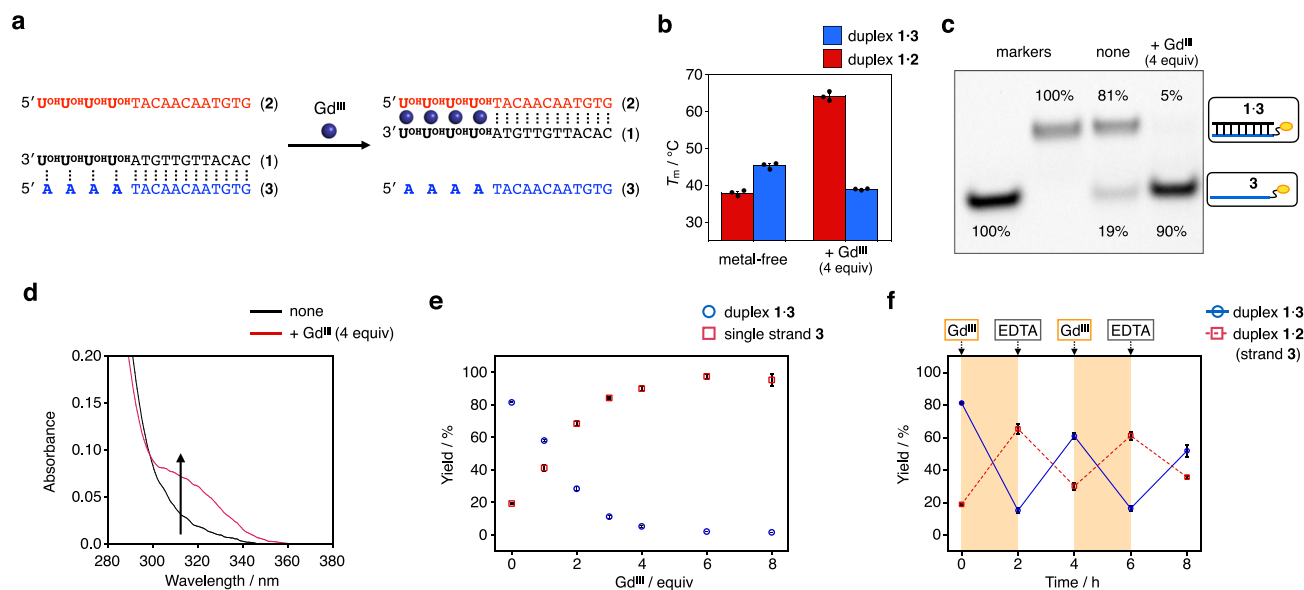


Fig. 2 | Metal-dependent regulation of the hybridization behavior of a DNA strand containing U^{OH} bases. **a** Schematic representation and base sequences. **b** Melting temperatures (T_m) of duplexes **1-2** (with U^{OH} - U^{OH} base pairs) and **1-3** (with U^{OH} -A base pairs) in the absence and presence of Gd^{III} ions (4 equiv). $N = 3$ independent experiments. Data are presented as mean values \pm SEM. **c** Native PAGE analysis of an equimolar mixture of strands **1**, **2**, and **3** in the absence and presence of Gd^{III} ions (4 equiv). The samples were annealed prior to the analysis. The strand **3** was labeled with FAM for detection. The authentic samples (strand **3** and pre-annealed duplex **1-3**) were employed as the markers. Three independent experiments were performed. **d** UV absorption spectra of the mixture at 25 °C. $l = 1$ cm.

The samples were annealed after the addition of Gd^{III} ions (4 equiv). **e** The yields of duplex **1-3** and single strand **3** in the presence of Gd^{III} ions at different concentrations. The yields were estimated by comparing the band intensities on the gel with those of the markers. $N = 3$ independent experiments. Data are presented as mean values \pm SEM. **f** Reversible regulation of the hybridization behaviors of U^{OH} -containing strand **1** by the alternate addition and removal of Gd^{III} ions under isothermal conditions (25 °C). $N = 4$ independent experiments. Data are presented as mean values \pm SEM. [DNA strand] = 2.0 μ M each, [$GdCl_3$] = 0 or 8.0 μ M (1 equiv per U^{OH} - U^{OH} pair, otherwise noted) in 10 mM HEPES (pH 8.0), 100 mM NaCl. Source data are provided as a Source Data file.

equiv and was little changed by the addition of excess Gd^{III} ions (Fig. 2e). These results show that hybridization preference of U^{OH} -containing strand **1** was changed in response to Gd^{III} .

Under isothermal conditions, sequential addition and removal of Gd^{III} ions resulted in reversible and alternating formation of duplexes **1-2** and **1-3** (Fig. 2f). Four equivalents of Gd^{III} ions and a chelating agent EDTA were added every 2 h at 25 °C. Native PAGE analysis of the hybridization products showed that the removal of Gd^{III} ions by EDTA induced the formation of duplex **1-3** containing U^{OH} -A pairs. Subsequent addition of Gd^{III} ions was found to regenerate duplex **1-2** via the interstrand U^{OH} - Gd^{III} - U^{OH} complexation. Thus, the hybridization partner of strand **1** containing U^{OH} bases was confirmed to be reversibly replaced by the addition and removal of Gd^{III} ions.

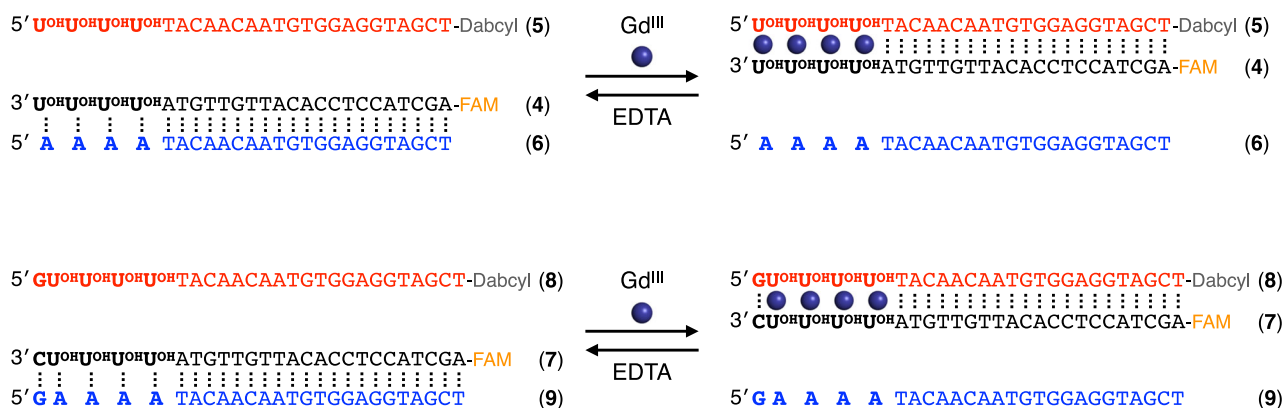
Based on these results, metal-triggered SDRs were investigated by using longer DNA strands (Fig. 3a). Since the starting duplex (**4-6** or **7-9**) is long enough, the SDR should proceed via binding of the invading strand (**5** or **8**) and subsequent branch migration process to replace the incumbent strand (**6** or **9**). Like strands **1-3**, strands **4** and **5** have four consecutive U^{OH} bases, and strand **6** has four A bases at their termini. Strands **7**, **8**, and **9** have an additional natural nucleotide (C or G) at the terminus to stabilize the duplexes. Even with the terminal G-C base pairs, the addition of Gd^{III} reversed the thermal stability of the duplex containing U^{OH} - U^{OH} pairs and the duplex containing U^{OH} -A pairs (Supplementary Fig. 6). To examine metal-mediated SDRs, 4 equiv of Gd^{III} ions were added to a mixture of a duplex containing U^{OH} -A base pairs (**4-6** or **7-9**) and a U^{OH} -modified invading strand (**5** or **8**, respectively). Two of the three strands (i.e., **4** and **5**, or **7** and **8**) were labeled with a fluorophore and a quencher, respectively. Thus, the progression of SDRs to form a duplex containing U^{OH} - Gd^{III} - U^{OH} base pairs (**4-5** or **7-8**) can be monitored by fluorescence quenching.

The results of the Gd^{III} -triggered SDRs are shown in Fig. 3b. The fluorescence decreased immediately after the addition of Gd^{III} ions,

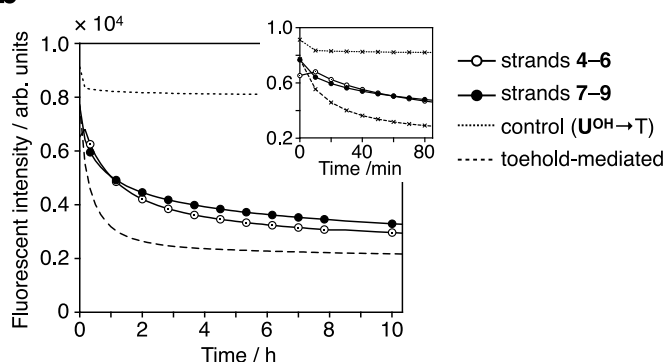
suggesting that SDR was initiated in response to Gd^{III} . The SDR proceeded at a similar rate regardless of the terminal G-C base pair. When the U^{OH} bases of strands **7** and **8** were replaced with natural T bases (**7t** and **8t**), little SDRs progressed with the addition of Gd^{III} ions. This result confirms that the SDRs were triggered by metal complexation of the U^{OH} bases, inducing base-pair switching from U^{OH} -A to U^{OH} - Gd^{III} - U^{OH} . Under these conditions, Gd^{III} -mediated SDRs were slower than conventional toehold-mediated SDRs^{8,9}. Complexation of U^{OH} - Gd^{III} - U^{OH} is completed within 1 min, as suggested by UV absorption analysis (Supplementary Fig. 7a). The results suggest that the subsequent branch migration is slowed down due to the structural distortion caused by U^{OH} - Gd^{III} - U^{OH} base pairing. In addition, the strand displacement may be delayed by the binding of the U^{OH} -modified invading strands (**5** or **8**) in a parallel orientation or by homodimerization of the invading strands via the U^{OH} - Gd^{III} - U^{OH} complexation (Supplementary Fig. 8). It is worth noting that the SDR using U^{OH} -containing strands is specifically triggered by certain lanthanide ions (Supplementary Fig. 9). The lanthanide ion Eu^{III} triggered the SDR as Gd^{III} does, while other transition metal ions such as Cu^{II} and Zn^{II} hardly induced SDR. The metal specificity is in good agreement with the fact that DNA duplexes containing U^{OH} - U^{OH} base pairs are stabilized only in the presence of lanthanide ions³⁰.

The addition of EDTA can remove Gd^{III} ions from the U^{OH} - Gd^{III} - U^{OH} base pairs inside the duplexes, although the demetallation reaction is slower than complexation (Supplementary Fig. 7b). Under Gd^{III} -free conditions, the SDR can be initiated by adding strand **9** containing AAAAG at the terminus to duplex **7-8** with U^{OH} - U^{OH} mismatches (Supplementary Fig. 10). Thus, it was expected that the addition of EDTA would induce SDRs from duplexes with U^{OH} - Gd^{III} - U^{OH} (**4-5** or **7-8**) to duplexes with U^{OH} -A pairs (**4-6** or **7-9**, respectively). When EDTA ([EDTA]/[Gd^{III}] = 1.0) was added to a mixture of a Gd^{III} -bridged duplex (**4-5** or **7-8**) and the other strand (**6** or **9**), the fluorescence was gradually

a



b



c

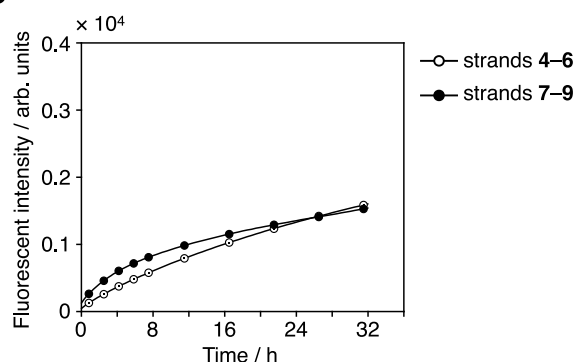


Fig. 3 | Metal-mediated DNA strand displacement reactions (SDRs) based on the base-pair switching of U^{OH} bases. **a** Design of metal-mediated SDRs. Strands 4 and 7 were labeled with a fluorophore (FAM) and strands 5 and 8 with a quencher (Dabcyl). **b** Time-course analysis of Gd^{III} -triggered SDRs. The reaction was started by the addition of Gd^{III} ions (4 equiv). In the control experiment, strands 7t and 8t, in which U^{OH} bases are replaced with natural T bases, were used instead of strands 7 and 8. The toehold-mediated reaction was carried out with FAM-labeled 7t, 8 s (21-

mer that lacks the terminal 5'- $\text{G}^{\text{U}^{\text{OH}}}\text{U}^{\text{OH}}\text{U}^{\text{OH}}\text{U}^{\text{OH}}$ 3'), and Dabcyl-labeled 9. **c** Time-course analysis of EDTA-triggered SDRs. The reaction was started by the addition of EDTA (4 equiv) to remove Gd^{III} ions. [DNA strand] = 2.0 μM each in 10 mM HEPES buffer (pH 8.0), 100 mM NaCl, 25 $^{\circ}\text{C}$. The SDRs were monitored by the changes in the fluorescence of the FAM. $\lambda_{\text{ex}} = 495 \text{ nm}$, $\lambda_{\text{em}} = 519 \text{ nm}$. Source data are provided as a Source Data file.

increased. This result indicates that SDRs proceeded in the reverse direction (Fig. 3c). The slow rate of the EDTA-induced SDRs could be improved by increasing the number of U^{OH} bases or by adding terminal bases only to the toehold and the incoming strand.

As discussed above, Gd^{III} -triggered SDRs using the U^{OH} base as a metal-binding site are now possible. Gd^{III} destabilized the $\text{U}^{\text{OH}}\text{-A}$ base pairs and induced the formation of the $\text{U}^{\text{OH}}\text{-Gd}^{\text{III}}\text{-U}^{\text{OH}}$ base pairs. This base-pair switching promoted the displacement of the A-containing incumbent strands with the U^{OH} -containing invading strand. The SDRs were found to proceed in the reverse direction upon removal of the Gd^{III} ions, which induces base-pair switching from $\text{U}^{\text{OH}}\text{-Gd}^{\text{III}}\text{-U}^{\text{OH}}$ to $\text{U}^{\text{OH}}\text{-A}$. Note that the SDRs developed in this study are reversible even though there are no exposed toehold regions in the strands. Since Gd^{III} ions are unlikely to interact with natural nucleobases, the Gd^{III} -triggered SDRs using unnatural U^{OH} nucleobases would have significant advantages, especially when integrated into cascade SDRs such as DNA computing circuits. Thus, SDRs based on the base-pair switching between $\text{U}^{\text{OH}}\text{-A}$ and $\text{U}^{\text{OH}}\text{-Gd}^{\text{III}}\text{-U}^{\text{OH}}$ may provide a useful strategy for designing a wide variety of stimuli-responsive DNA molecular systems.

Development of metal-responsive DNA tweezers using U^{OH} bases

Based on the results of the strand displacement experiments, we further applied the U^{OH} bases to the development of metal-responsive

DNA molecular devices. As the simplest model, a pair of DNA tweezers^{28,38–40} was created that switch its structure upon metal complexation of the U^{OH} bases (Fig. 4a). DNA tweezers are nanodevices consisting of two arms that take two forms, closed and open. Despite their simple structure, DNA tweezers have been applied to capture target proteins⁴¹ and regulate enzyme functions⁴², making them an important prototype of DNA molecular machines. The base sequence of the metal-responsive tweezers was designed based on Yurke's original DNA tweezers²⁸ operated by toehold-mediated SDR using fuel strands (Fig. 4b). The tweezers consist of two DNA duplex arms connected by a single-strand hinge. Hybridization of complementary oligonucleotides (strand **d**) at both dangling ends locks the DNA tweezers into a closed state. The U^{OH} bases were introduced into strand **d** so that the tweezers are closed by $\text{U}^{\text{OH}}\text{-A}$ base pairing. The addition of Gd^{III} ions was expected to destabilize the $\text{U}^{\text{OH}}\text{-A}$ base pairs and to induce the release of strand **d** associated with the intramolecular $\text{U}^{\text{OH}}\text{-Gd}^{\text{III}}\text{-U}^{\text{OH}}$ base pairing, which would open the tweezers.

The structure of the U^{OH} -modified DNA tweezers was first evaluated by native PAGE analysis (Fig. 4c). Each band was characterized by comparing with the mobility of reference samples in which U^{OH} bases were replaced with T bases. When all strands were analyzed in the absence of Gd^{III} ions, a band corresponding to the closed state was mainly observed. In the presence of Gd^{III} ions, a new band with higher

Development of metal-dependent allosteric DNAzymes using U^{OH} bases

Deoxyribozymes (DNAzymes) are DNA oligomers with catalytic activity that were originally obtained by an in vitro selection method (SELEX) using nucleic acid libraries with a random sequence²⁹. Among a variety of DNAzymes, RNA-cleaving DNAzymes, which cleave oligonucleotide substrates containing a ribonucleotide, are widely used to construct DNA molecular machines and computing circuits^{43,44}. Allosteric regulation of DNAzyme activity is of growing interest as a promising strategy for constructing stimuli-responsive DNA systems⁴⁵. We have previously synthesized Cu^{II} -responsive allosteric DNAzymes by introducing metal-mediated artificial base pairs ($\text{H-Cu}^{\text{II}}\text{-H}$ or $\text{Im}^{\text{C}}\text{-Cu}^{\text{II}}\text{-Im}^{\text{C}}$) that stabilize DNA duplexes only in the presence of specific metal ions^{46–50}. Here, we developed a metal-responsive allosteric DNAzyme by applying a base-pair switching system between hydrogen-bonded $\text{U}^{\text{OH}}\text{-A}$ base pairs and metal-mediated $\text{U}^{\text{OH}}\text{-Gd}^{\text{III}}\text{-U}^{\text{OH}}$ base pairs (Fig. 5a).

The metal-responsive DNAzyme was designed based on the secondary structure of the RNA-cleaving NaA43 DNAzyme reported previously⁵¹ (Fig. 5b). Three $\text{U}^{\text{OH}}\text{-U}^{\text{OH}}$ base pairs were incorporated into the stem duplex as metal-binding sites. The sequence of the surrounding bases was modified to form a catalytically inactive structure with $\text{U}^{\text{OH}}\text{-A}$ base pairs in the absence of Gd^{III} ions. The addition of Gd^{III} ions was expected to switch the base pairing from $\text{U}^{\text{OH}}\text{-A}$ to $\text{U}^{\text{OH}}\text{-Gd}^{\text{III}}\text{-U}^{\text{OH}}$, resulting in a structure transformation from the inactive to the catalytically active form.

The RNA-cleaving activity of the U^{OH} -modified DNAzyme (named as U^{OH} -DNAzyme) was evaluated in the absence and presence of Gd^{III} ions. The reaction was initiated by the addition of a fluorophore-labeled substrate (10 equiv), and the time course of the reaction was monitored by denaturing PAGE (Fig. 5c). In the absence of Gd^{III} ions, the activity of U^{OH} -DNAzyme was efficiently suppressed ($k_{\text{obs}} = 4.8 \times 10^{-3} \text{ h}^{-1}$) compared to that of the original NaA43 DNAzyme ($4.2 \times 10^{-1} \text{ h}^{-1}$). This result indicates that the U^{OH} -DNAzyme adopted a

catalytically inactive structure in the absence of Gd^{III} ions. The addition of 3 equiv of Gd^{III} ions enhanced the catalytic reaction of U^{OH} -DNAzyme ($k_{\text{obs}} = 6.9 \times 10^{-2} \text{ h}^{-1}$). The activity of the unmodified DNAzyme was also increased by the addition of Gd^{III} ions ($k_{\text{Gd}^{\text{III}}}/k_{\text{Gd}^{\text{III}}-} = 1.9$), but the Gd^{III} -induced activity enhancement of the U^{OH} -DNAzyme was much more pronounced ($k_{\text{Gd}^{\text{III}}}/k_{\text{Gd}^{\text{III}}-} = 14.4$). These results show that the interactions between U^{OH} and Gd^{III} play a pivotal role in DNAzyme activation. In control experiments using T-DNAzyme, in which all U^{OH} bases were replaced with thymine (T) bases, no substrate cleavage was observed in the presence of Gd^{III} ions, suggesting that U^{OH} -DNAzyme was activated by the complexation of U^{OH} bases with Gd^{III} ions. UV spectroscopy also revealed the appearance of a new absorption band around 310 nm by the addition of Gd^{III} ions (Supplementary Fig. 11), suggesting metal complexation of the U^{OH} bases^{30,31}. It can be concluded that the activity of U^{OH} -DNAzyme is allosterically enhanced by the formation of $\text{U}^{\text{OH}}\text{-Gd}^{\text{III}}\text{-U}^{\text{OH}}$ base pairs, stabilizing the catalytically active structure. It should also be noted that the U^{OH} -DNAzyme showed more efficient switching capability ($k_{\text{Gd}^{\text{III}}}/k_{\text{Gd}^{\text{III}}-} = 14.4$) than the Cu^{II} -responsive DNAzyme ($k_{\text{Cu}^{\text{II}}}/k_{\text{Cu}^{\text{II}}-} = 5.9$)⁴⁷ developed by incorporating an $\text{H-Cu}^{\text{II}}\text{-H}$ base pair into the same parent DNAzyme. This is thought to be due to a unique design strategy based on the bifacial nature of the U^{OH} bases, whereby the inactive secondary structure (with $\text{U}^{\text{OH}}\text{-A}$ base pairs) and the active structure (with $\text{U}^{\text{OH}}\text{-Gd}^{\text{III}}\text{-U}^{\text{OH}}$ pairs) are formed stably in the absence and presence of Gd^{III} ions, respectively.

We found that the DNAzyme activity during the reaction can be controlled by adding and removing Gd^{III} ions. The substrate was treated with U^{OH} -DNAzyme in the absence of Gd^{III} ions for 2 h, and then Gd^{III} ions were added. Time-course analysis showed that the addition of Gd^{III} ions increased the DNAzyme activity to the level observed with Gd^{III} ions from the beginning (Fig. 5d). When the chelating agent EDTA was added to remove Gd^{III} ions, U^{OH} -DNAzyme was immediately inactivated (Fig. 5e). It is interesting to note that the DNAzyme activity changed a short time after the addition or removal of Gd^{III} ions. This is probably because the intramolecular structure transformation requires a little time.

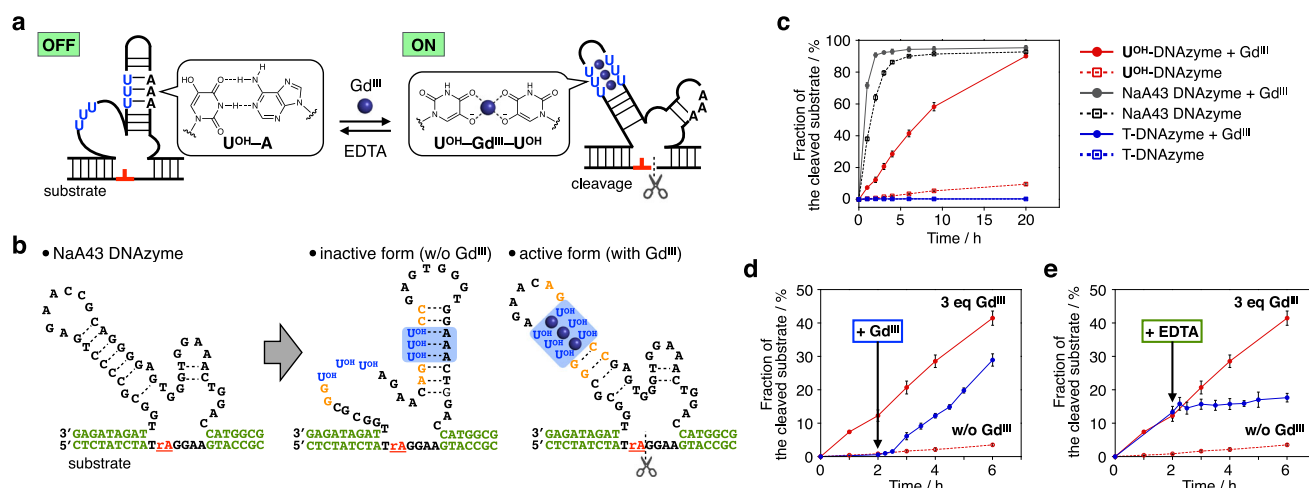


Fig. 5 | Development of a Gd^{III} -responsive allosteric DNAzyme based on the base-pair switching of U^{OH} bases. **a Schematic representation of the Gd^{III} -responsive allosteric DNAzyme. U represents U^{OH} nucleotides. **b** Base sequence of the U^{OH} -modified DNAzyme (U^{OH} -DNAzyme). DNA strands containing an adenosine ribonucleotide (rA) at the cleavage site were used as the substrate. Both the catalytically inactive form (without Gd^{III}) and the active form (with Gd^{III}) are shown. The original NaA43 DNAzyme was modified by introducing U^{OH} bases, and surrounding nucleobases (shown in orange) were further altered to stabilize the inactive structure in the absence of Gd^{III} ions. **c** RNA-cleaving activity of U^{OH} -DNAzyme, the original NaA43 DNAzyme, and T-DNAzyme in the absence and presence of Gd^{III} ions (3 equiv). $N = 3$ (for U^{OH} -DNAzyme) and $N = 4$ (for the others) independent experiments. Data are presented as mean values \pm SEM. T-DNAzyme has T bases in place**

of U^{OH} bases, thus lacking the metal binding affinity. The substrate cleavage was analyzed by denaturing PAGE using a substrate labeled with a fluorophore (FAM). **d** Activation of U^{OH} -DNAzyme by the addition of Gd^{III} ions (3 equiv). The activity of U^{OH} -DNAzyme in the presence and absence of Gd^{III} ions (3 equiv) is also shown by the red lines. $N = 3$ independent experiments. Data are presented as mean values \pm SEM. **e** Deactivation of U^{OH} -DNAzyme by removing Gd^{III} ions. An equimolar amount of EDTA was added to remove the Gd^{III} ions. $N = 4$ independent experiments. Data are presented as mean values \pm SEM. [U^{OH} -DNAzyme] = 1.0 μM , [substrate] = 10 μM , [GdCl_3] = 3.0 μM (3 equiv, where applicable), [EDTA] = 3.0 μM (3 equiv, where applicable) in 10 mM HEPES (pH 7.0), 100 mM NaCl, 25 $^\circ\text{C}$. Source data are provided as a Source Data file.

All results presented here show that the activity of U^{OH} -DNAzyme is allosterically regulated in response to Gd^{III} ions under isothermal conditions. This is due to molecular design based on the base-pair switching between $\text{U}^{\text{OH}}\text{-A}$ and $\text{U}^{\text{OH}}\text{-Gd}^{\text{III}}\text{-U}^{\text{OH}}$. Although the duplex structure around the $\text{U}^{\text{OH}}\text{-Gd}^{\text{III}}\text{-U}^{\text{OH}}$ base pairs is presumed to be distorted³⁰, the U^{OH} -modified DNAzyme showed catalytic activity in the presence of Gd^{III} ions. Note that U^{OH} bases served as metal-responsive switches to induce DNA structural conversion even when located at internal positions. Sequence design based on the base-pair switching of U^{OH} may be applicable not only to allosteric DNAzymes but also to the development of various metal-responsive functional DNA devices.

Discussion

In this study, we have shown that Gd^{III} -dependent DNA nanostructure transformation is possible by base-pair switching between hydrogen-bonded $\text{U}^{\text{OH}}\text{-A}$ base pairs and metal-mediated $\text{U}^{\text{OH}}\text{-Gd}^{\text{III}}\text{-U}^{\text{OH}}$ base pairs. In the absence of Gd^{III} ions, U^{OH} forms $\text{U}^{\text{OH}}\text{-A}$ base pairs, which are similar to Watson-Crick T-A pairs. When Gd^{III} ions are added as external stimuli, the $\text{U}^{\text{OH}}\text{-A}$ base pair is destabilized and the $\text{U}^{\text{OH}}\text{-Gd}^{\text{III}}\text{-U}^{\text{OH}}$ base pairs can be preferentially formed instead. The addition and removal of Gd^{III} ions result in the exchange of hybridization partners of the U^{OH} -containing strands even under isothermal conditions. The introduction of multiple U^{OH} bases at the termini of DNA strands enabled a Gd^{III} -triggered strand displacement reaction (SDR), although it is not as fast as standard toehold-mediated SDRs. This metal-responsive SDR is reversible and does not require any toehold sequences, making it a versatile approach to creating dynamic DNA molecular devices.

The Gd^{III} -mediated base-pair switching was further applied to the operation of DNA tweezers as a simple model for DNA molecular devices. Gel electrophoresis and FRET analysis confirmed that the DNA tweezers repeatedly open and close in response to Gd^{III} ions. We also confirmed that this method can be applied to control the activity of a catalytic DNA (DNAzyme). Here, we designed a Gd^{III} -dependent transformation between a catalytically inactive structure containing $\text{U}^{\text{OH}}\text{-A}$ base pairs and an active structure with $\text{U}^{\text{OH}}\text{-Gd}^{\text{III}}\text{-U}^{\text{OH}}$ base pairs. As a result, we succeeded in activating and inactivating the DNAzyme in response to the metal. Thus, U^{OH} nucleobases are expected to be widely applied to manipulate DNA molecular devices and machines using metal ions as external stimuli.

The use of metal ions as external stimuli in dynamic DNA nanotechnology has the following characteristics. (1) Because coordination bonds are generally more stable than hydrogen bonds, metal-mediated base pairing can significantly alter the stability of DNA duplexes²³. This is advantageous for inducing strand displacement and structure transformation of DNA constructs. (2) Metal coordination is fundamentally reversible, allowing repeated manipulation of metal-DNA systems, as demonstrated with the DNA tweezers in this study. Reversible SDRs could be useful in developing advanced DNA computing circuits. (3) A wide variety of metal ions are available for this purpose, and equimolar amounts or small excesses of metal ions are sufficient as stimuli when suitable ligands are used. Multiple metal species can also be used as orthogonal stimuli based on specific interactions between metal ions and ligands^{46,48}. (4) SDRs triggered by biologically relevant metal ions have a wide range of biological applications.

Metal-mediated base pairs composed of natural nucleobases (i.e., T-Hg^{II}-T and C-Ag^I-C)⁵²⁻⁵⁵ have been used to construct metal-responsive DNA devices. However, these metal ions can bind to T and C bases at undesired positions that are difficult to predict, making sequence design not easy. We have worked to rationally design metal-responsive DNA supramolecules by introducing metal-mediated base pairs with unnatural ligand-type nucleobases⁴⁶⁻⁵⁰. Compared to these conventional approaches, metal-mediated base-pair switching dramatically alters duplex stability and hybridization behavior, making it

suitable for dynamic control of DNA nanostructures. Moreover, because only modified nucleotides were used as additional building blocks, the strategies presented here are highly compatible with standard DNA nanotechnologies.

The basic behaviors seen in the metal-mediated SDRs and DNA nanodevice presented here are based on the unique concept of metal-mediated base-pair switching of modified pyrimidine bases. In conventional pH-responsive¹⁰ and light-responsive systems¹¹⁻¹³, only (de)hybridization of DNA strands is controlled by external stimuli. In contrast, our approach can reversibly switch two different states: a structure with $\text{U}^{\text{OH}}\text{-A}$ base pairs (i.e., inactive state) and one with $\text{U}^{\text{OH}}\text{-Gd}^{\text{III}}\text{-U}^{\text{OH}}$ base pairs (active state), as clearly demonstrated using the U^{OH} -DNAzyme. These features provide a useful basis for the development of DNA nanodevices, molecular machines, computing circuits, and more advanced systems⁵⁶. In contrast to the selection methods by which various metal-dependent DNAzymes have been found⁵⁷, our strategy is primarily focused on the rational design of metal-responsive DNA materials. Modification of existing functional DNAs is also a suitable approach, as the DNA sequences can be easily designed by replacing natural T bases with U^{OH} bases. U^{OH} nucleoside and U^{OH} -modified oligonucleotides are readily available, and U^{OH} bases function as metal-triggered switches not only at the termini of the DNA strands but also internally. Therefore, the U^{OH} bases will be a useful building block for designing metal-responsive dynamic DNA architectures.

It should also be mentioned that metal-mediated SDR at lower concentrations is required for practical application in DNA nanotechnology. Because of the potential interaction of Gd^{III} ions with phosphate groups, the use of other metal ions that rarely interact with natural DNA may be more appropriate for applications in complex systems consisting of many DNA strands. Metal-mediated base-pair switching can also be possible with other 5-substituted pyrimidine bases such as 5-carboxyuracil (**caU**)⁵⁸ and *N,N*-dicarboxymethyl-5-aminouracil (**dcaU**)⁵⁹, both of which were found to form more stabilizing metal-mediated base pairs (**caU**-Cu^I-**caU** and **dcaU**-Gd^{III}-**dcaU**) as well as hydrogen-bonded base pairs (**caU**-A and **dcaU**-A). We believe that this method can be extended to other metal ions by designing bifacial nucleobases with different coordination functionality at the 5-position or by modifying cytosine bases. Thus, the principle of metal-mediated base-pair switching appears to be a versatile approach that extends the scope of dynamic DNA nanotechnology. The application of these bifacial nucleobases to the metal-dependent reconfiguration of DNA nanostructures is currently under investigation in our laboratory.

Methods

Materials and equipment

All natural DNA strands, including FAM-labeled strands, Dabcyl-labeled strands, and substrate strands containing a riboadenosine (rA) were purchased from Japan Bio Service Co., Ltd. (Saitama, Japan) at HPLC purification grade. The sequences of the DNA strands used in this study are summarized in Supplementary Table 1. Oligonucleotide concentrations were determined based on UV absorbance at 260 nm. $\text{GdCl}_3 \cdot 6\text{H}_2\text{O}$ (99.9% purity) purchased from Soekawa Chemical Co. was used as a metal source without further purification. The gels were analyzed using Gel Doc EZ Imager and Image Lab software ver. 6.1.0 (Bio-Rad). All the graphs were produced by KaleidaGraph ver. 5.0.3 (HULINKS).

DNA synthesis

DNA strands containing 5-hydroxyuracil (U^{OH}) nucleobases were synthesized on an automated DNA synthesizer (NTS M-2-MX DNA/RNA synthesizer)³⁰. The DNA synthesis was carried out on a 1- μmol scale in a DMTr-on mode with ultramild deprotection phosphoramidites and reagents (Glen Research). Note that the phosphoramidite monomer of U^{OH} deoxynucleoside was synthesized following the literature^{60,61} or

purchased from Glen Research (catalog No. 10-1053). The coupling time of U^{OH} was extended to 15 min. The products were deprotected using 28% NH_3 aqueous solution at room temperature for 2–3 h and then purified and detritylated using a PolyPak II cartridge (Glen Research). Some of the U^{OH} -containing strands were prepared by the ligation of a shorter U^{OH} -containing strand and a natural strand by using a T4 DNA ligase. The oligonucleotides were purified by reverse-phase HPLC (Waters XBridge C18 column) or by denaturing polyacrylamide gel electrophoresis. All DNA strands were identified by MALDI-TOF or ESI-TOF mass spectrometry (Supplementary Table 2).

Duplex melting analysis

The samples were prepared by mixing the DNA strands (2 μM) in 10 mM HEPES buffer (pH 8.0) containing 100 mM NaCl. After the addition of Gd^{III} ions (0–6 equiv), the solutions were heated to 85 °C and cooled slowly to 4 °C at a rate of -1.0 °C/min. Absorbance at 260 nm was monitored by UV-1800 and UV-1900 spectrophotometers (Shimadzu) equipped with a TMSPC-8 temperature controller while the temperature was raised from 4 to 85 °C at a rate of 0.2 °C/min. Normalized absorbance shown in the figures was calculated as follows:

$$\text{Normalized } \Delta A_{260} = \{A_{260}(t\text{ }^\circ\text{C}) - A_{260}(4\text{ }^\circ\text{C})\} / \{A_{260}(85\text{ }^\circ\text{C}) - A_{260}(4\text{ }^\circ\text{C})\}. \quad (1)$$

The melting temperature (T_m) was determined as the inflection point of the melting curve using LabSolutions T_m analysis software ver. 1.40 (Shimadzu) with a 17-point adaptive smoothing program. The average T_m values of at least three independent runs were calculated.

Mass spectrometry of the DNA duplexes

Electrospray ionization-time-of-flight (ESI-TOF) mass spectra were recorded on a Waters Micromass LCT premier. The samples (40 μM) were prepared in 20 mM NH_4OAc buffer (pH 7.0) and annealed just before the measurements (from 85 to 4 °C, -1.0 °C/min).

Metal-dependent regulation of the hybridization behavior of U^{OH} -containing DNA strands

Strand **3** was labeled with FAM. The samples were prepared by mixing the DNA strands (2 μM each) in 10 mM HEPES buffer (pH 8.0) containing 100 mM NaCl. The solutions were annealed (85 °C \rightarrow 4 °C, -1.0 °C/min) in the absence or presence of Gd^{III} ions. For the reversible regulation shown in Fig. 2f, after the solutions were annealed (85 °C \rightarrow 25 °C, -1.0 °C/min), GdCl_3 (4 equiv) and EDTA (4 equiv) were alternately added every 2 h at 25 °C. Native gel electrophoresis was carried out with 20% polyacrylamide gel in a cool incubator (4 °C). The bands were detected by FAM fluorescence, and the yield of each product was calculated by comparing the band intensities of the authentic samples on the same gel. The averages of at least three runs are summarized. The gel shown in Supplementary Fig. 5 was stained with SYBR Gold. The UV spectra of the samples were also recorded at 5 °C on a JASCO V-730 spectrometer.

Metal-mediated DNA strand displacement reactions (SDRs)

Strands **4** and **7** were labeled with a fluorophore (FAM) and strands **5** and **8** with a quencher (Dabcyl). The initial duplexes (**4-6** or **7-9** for Gd^{III} -triggered reaction, and **4-5** or **7-8** for EDTA-triggered reaction) were prepared by combining the two strands (2.0 μM each) in 10 mM HEPES buffer (pH 8.0) containing 100 mM NaCl in the absence or presence of Gd^{III} ions (4 equiv). After annealing from 85 to 25 °C (-1.0 °C/min), the mixture was kept at 25 °C. After the addition of the other strand, the SDR was initiated by the addition of Gd^{III} ions (4 equiv) or EDTA (4 equiv). The reaction progress was monitored by the changes in the fluorescence intensity of the FAM ($\lambda_{\text{ex}} = 495$ nm, $\lambda_{\text{em}} = 519$ nm) using an FP-8350 fluorometer (JASCO). The fluorescent intensity was recorded in 10-min intervals for 8 h and subsequently in 30-min intervals. In the

control experiments, the toehold-mediated SDR was started by adding the invading strands to the pre-annealed duplex. In the metal selectivity test (Supplementary Fig. 9), the fluorescence intensity ($\lambda_{\text{ex}} = 495$ nm, $\lambda_{\text{em}} = 520$ nm) was recorded on a Varioskan LUX plate-reader (Thermo Fisher).

Metal-mediated operation of the DNA tweezers

Strand **b** was labeled with FAM at the 5' end for native PAGE analysis or with FAM and Dabcyl at both termini for FRET analysis. The samples were prepared by combining DNA strands **a**, **b**, **c**, and **d** (2 μM each) in 10 mM HEPES buffer (pH 8.0) containing 100 mM NaCl and 3 mM MgCl_2 . The solutions were annealed (85 °C \rightarrow 25 °C, -1.0 °C/min) in the absence or presence of Gd^{III} ions (4, 8, 12, and 20 equiv). Native PAGE was carried out with 15% polyacrylamide gel in an incubator (20 °C). The bands were detected by FAM fluorescence, and the yields of the closed and the open states were estimated by comparing the band intensities. The averages of at least three runs are summarized. A mixture of strands **a**, **b**, and **c** was used as a marker corresponding to the open state. A mixture of strands **a**, **b**, **c**, and **d'**, in which U^{OH} nucleotides were replaced with T, was used to indicate the closed state. For the FRET analysis, the fluorescence spectra were measured at 25 °C ($\lambda_{\text{ex}} = 495$ nm).

Time-course study of the operation of the DNA tweezers

Strand **b** was labeled with FAM and Dabcyl at both termini. DNA strands **a**, **b**, **c**, and **d** (2 μM each) were mixed in 10 mM HEPES buffer (pH 8.0) containing 100 mM NaCl and 3 mM MgCl_2 . The mixtures were annealed (85 °C \rightarrow 25 °C, -1.0 °C/min) in the absence or presence of Gd^{III} ions (12 equiv). Gd^{III} ions (12 equiv) or EGTA (12 equiv) were added while maintaining 25 °C. The change in the fluorescence intensity was monitored in 30-s intervals at 25 °C ($\lambda_{\text{ex}} = 495$ nm, $\lambda_{\text{em}} = 519$ nm). In the control experiments, strand **d** was added to the pre-annealed mixture of strands **a**, **b**, and **c**.

Repetitive opening and closing of the tweezers

The sample was prepared in the absence of Gd^{III} ions, as described above. With keeping the temperature at 25 °C, Gd^{III} ions (12 equiv) or EGTA (12 equiv) were alternately added at the defined time points. The reaction progress was monitored by native PAGE and FRET analysis.

Metal-mediated regulation of DNAzyme activity

A DNAzyme strand (1.0 μM) was annealed (85 °C \rightarrow 25 °C, -1.0 °C/min) in a reaction buffer (10 mM HEPES (pH 7.0), 100 mM NaCl) in the presence or absence of GdCl_3 (3 equiv). The RNA-cleaving reaction was initiated by adding a FAM-labeled substrate (10 equiv). After incubating at 25 °C, the reaction was stopped by adding a 3:1 mixture of 7 M urea and the loading buffer. The progress of the DNAzyme reaction was analyzed by denaturing PAGE. The percentage of the cleaved product (F) was calculated as follows:

$$F(\%) = I_c / (I_c + I_u) \times 100, \quad (2)$$

where I_c and I_u are the band intensities of the cleaved and the uncleaved substrate, respectively. The apparent first-order rate constants (k_{obs}) were calculated from the initial velocity determined from the time points when F was less than 20%.

Regulation of DNAzyme activity during the reaction

For the Gd^{III} -triggered DNAzyme activation, the RNA-cleaving reaction was initiated in the absence of Gd^{III} ions. After 2 h, GdCl_3 (3 equiv) was added. For the deactivation by the removal of Gd^{III} ions, the reaction was started in the presence of Gd^{III} ions (3 equiv). After 2 h, a chelating agent EDTA (3 equiv) was added to remove Gd^{III} ions. The reaction progress was monitored by denaturing PAGE as described above.

Reporting summary

Further information on research design is available in the Nature Portfolio Reporting Summary linked to this article.

Data availability

All the data supporting the results of this study are available in this paper and the Supplementary Information. Source data are provided with this paper.

References

- Seeman, N. C. & Sleiman, H. F. DNA nanotechnology. *Nat. Rev. Mater.* **3**, 17068 (2017).
- Seeman, N. C. *Structural DNA Nanotechnology* (Cambridge University Press, 2016).
- Dey, S. et al. DNA origami. *Nat. Rev. Methods Primers* **1**, 13 (2021).
- Hong, F., Zhang, F., Liu, Y. & Yan, H. DNA origami: scaffolds for creating higher order structures. *Chem. Rev.* **117**, 12584–12640 (2017).
- DeLuca, M., Shi, Z., Castro, C. E. & Arya, G. Dynamic DNA nanotechnology: toward functional nanoscale devices. *Nanoscale Horiz.* **5**, 182–201 (2020).
- Zhang, Y. et al. Dynamic DNA structures. *Small* **15**, e1900228 (2019).
- Wang, F., Liu, X. & Willner, I. DNA switches: from principles to applications. *Angew. Chem. Int. Ed. Engl.* **54**, 1098–1129 (2015).
- Zhang, D. Y. & Seelig, G. Dynamic DNA nanotechnology using strand displacement reactions. *Nat. Chem.* **3**, 103–113 (2011).
- Simmel, F. C., Yurke, B. & Singh, H. R. Principles and applications of nucleic acid strand displacement reactions. *Chem. Rev.* **119**, 6326–6369 (2019).
- Mattath, M. N., Ghosh, D., Pratihari, S., Shi, S. & Govindaraju, T. Nucleic acid architectonics for pH-responsive DNA systems and devices. *ACS Omega* **7**, 3167–3176 (2022).
- Wang, C. et al. Photoresponsive DNA materials and their applications. *Chem. Soc. Rev.* **51**, 720–760 (2022).
- Lubbe, A. S., Szymanski, W. & Feringa, B. L. Recent developments in reversible photoregulation of oligonucleotide structure and function. *Chem. Soc. Rev.* **46**, 1052–1079 (2017).
- Kamiya, Y. & Asanuma, H. Light-driven DNA nanomachine with a photoresponsive molecular engine. *Acc. Chem. Res.* **47**, 1663–1672 (2014).
- Yang, H., Liu, H., Kang, H. & Tan, W. Engineering target-responsive hydrogels based on aptamer-target interactions. *J. Am. Chem. Soc.* **130**, 6320–6321 (2008).
- Zhang, Q.-L., Wang, L.-L., Liu, Y., Lin, J. & Xu, L. A kinetically controlled platform for ligand-oligonucleotide transduction. *Nat. Commun.* **12**, 4654 (2021).
- Madsen, M. & Gothelf, K. V. Chemistries for DNA nanotechnology. *Chem. Rev.* **119**, 6384–6458 (2019).
- Krissanaprasit, A., Key, C. M., Pontula, S. & LaBean, T. H. Self-assembling nucleic acid nanostructures functionalized with aptamers. *Chem. Rev.* **121**, 13797–13868 (2021).
- Ranallo, S., Sorrentino, D. & Ricci, F. Orthogonal regulation of DNA nanostructure self-assembly and disassembly using antibodies. *Nat. Commun.* **10**, 5509 (2019).
- McConnell, A. J., Wood, C. S., Neelakandan, P. P. & Nitschke, J. R. Stimuli-responsive metal-ligand assemblies. *Chem. Rev.* **115**, 7729–7793 (2015).
- Champin, B., Mobian, P. & Sauvage, J.-P. Transition metal complexes as molecular machine prototypes. *Chem. Soc. Rev.* **36**, 358–366 (2007).
- Durot, S., Heitz, V., Sour, A. & Sauvage, J.-P. Transition-metal-complexed catenanes and rotaxanes: from dynamic systems to functional molecular machines. *Top. Curr. Chem.* **354**, 35–70 (2014).
- Goswami, A., Saha, S., Biswas, P. K. & Schmittel, M. (Nano) mechanical motion triggered by metal coordination: from functional devices to networked multicomponent catalytic machinery. *Chem. Rev.* **120**, 125–199 (2020).
- Mergny, J.-L. & Sen, D. DNA quadruple helices in nanotechnology. *Chem. Rev.* **119**, 6290–6325 (2019).
- Tanaka, Y. et al. Structures, physicochemical properties, and applications of T-Hg^{II}-T, C-Ag^I-C, and other metallo-base-pairs. *Chem. Commun.* **51**, 17343–17360 (2015).
- Takezawa, Y., Müller, J. & Shionoya, M. Artificial DNA base pairing mediated by diverse metal ions. *Chem. Lett.* **46**, 622–633 (2017).
- Takezawa, Y. & Shionoya, M. Metal-mediated DNA base pairing: alternatives to hydrogen-bonded Watson-Crick base pairs. *Acc. Chem. Res.* **45**, 2066–2076 (2012).
- Müller, J. Nucleic acid duplexes with metal-mediated base pairs and their structures. *Coord. Chem. Rev.* **393**, 37–47 (2019).
- Yurke, B., Turberfield, A. J., Mills, A. P., Simmel, F. C. & Neumann, J. L. A DNA-fuelled molecular machine made of DNA. *Nature* **406**, 605–608 (2000).
- Ma, L. & Liu, J. Catalytic nucleic acids: biochemistry, chemical biology, biosensors, and nanotechnology. *iScience* **23**, 100815 (2020).
- Takezawa, Y., Nishiyama, K., Mashima, T., Katahira, M. & Shionoya, M. Bifacial base-pairing behaviors of 5-hydroxyuracil DNA bases through hydrogen bonding and metal coordination. *Chem. Eur. J.* **21**, 14713–14716 (2015).
- Nishiyama, K., Mori, K., Takezawa, Y. & Shionoya, M. Metal-responsive reversible binding of triplex-forming oligonucleotides with 5-hydroxyuracil nucleobases. *Chem. Commun.* **57**, 2487–2490 (2021).
- Nishiyama, K., Takezawa, Y. & Shionoya, M. pH-dependence of the thermal stability of metallo-DNA duplexes containing ligand-type 5-hydroxyuracil nucleobases. *Inorg. Chim. Acta* **452**, 176–180 (2016).
- Amodio, A. et al. Rational design of pH-controlled DNA strand displacement. *J. Am. Chem. Soc.* **136**, 16469–16472 (2014).
- Morihiro, K., Kodama, T., Waki, R. & Obika, S. Light-triggered strand exchange reaction using the change in the hydrogen bonding pattern of a nucleobase analogue. *Chem. Sci.* **5**, 744–750 (2014).
- Kou, B., Zhang, J., Huai, X., Liang, X. & Xiao, S.-J. Light-driven reversible strand displacement using glycerol azobenzene inserted DNA. *RSC Adv.* **5**, 5055–5058 (2015).
- Wang, L.-L. et al. Controllable DNA strand displacement by independent metal-ligand complexation. *Chem. Sci.* **12**, 8698–8705 (2021).
- Ding, W., Deng, W., Zhu, H. & Liang, H. Metallo-toeholds: controlling DNA strand displacement driven by Hg(II) ions. *Chem. Commun.* **49**, 9953–9955 (2013).
- Liu, M. et al. A DNA tweezer-actuated enzyme nanoreactor. *Nat. Commun.* **4**, 2127 (2013).
- Liang, X., Nishioka, H., Takenaka, N. & Asanuma, H. A DNA nanomachine powered by light irradiation. *ChemBioChem* **9**, 702–705 (2008).
- Elbaz, J., Wang, Z.-G., Orbach, R. & Willner, I. pH-stimulated concurrent mechanical activation of two DNA “tweezers”. A “SET-RESET” logic gate system. *Nano Lett.* **9**, 4510–4514 (2009).
- Zhou, C., Yang, Z. & Liu, D. Reversible regulation of protein binding affinity by a DNA machine. *J. Am. Chem. Soc.* **134**, 1416–1418 (2012).
- Hu, Y. et al. Switchable enzyme/DNAzyme cascades by the reconfiguration of DNA nanostructures. *Chem. Eur. J.* **20**, 16203–16209 (2014).
- Liu, M., Chang, D. & Li, Y. Discovery and biosensing applications of diverse RNA-cleaving DNAzymes. *Acc. Chem. Res.* **50**, 2273–2283 (2017).
- Orbach, R., Willner, B. & Willner, I. Catalytic nucleic acids (DNAzymes) as functional units for logic gates and computing circuits: from basic principles to practical applications. *Chem. Commun.* **51**, 4144–4160 (2015).

45. Huang, Z., Wang, X., Wu, Z. & Jiang, J.-H. Recent advances on DNAzyme-based sensing. *Chem. Asian J.* **17**, e2021014 (2022).
46. Takezawa, Y., Nakama, T. & Shionoya, M. Enzymatic synthesis of Cu(II)-responsive deoxyribozymes through polymerase incorporation of artificial ligand-type nucleotides. *J. Am. Chem. Soc.* **141**, 19342–19350 (2019).
47. Nakama, T., Takezawa, Y., Sasaki, D. & Shionoya, M. Allosteric regulation of DNAzyme activities through intrastrand transformation induced by Cu(II)-mediated artificial base pairing. *J. Am. Chem. Soc.* **142**, 10153–10162 (2020).
48. Takezawa, Y., Hu, L., Nakama, T. & Shionoya, M. Sharp switching of DNAzyme activity through the formation of a Cu(II)-mediated carboximidazole base pair. *Angew. Chem. Int. Ed. Engl.* **59**, 21488–21492 (2020).
49. Nakama, T., Takezawa, Y. & Shionoya, M. Site-specific polymerase incorporation of consecutive ligand-containing nucleotides for multiple metal-mediated base pairing. *Chem. Commun.* **57**, 1392–1395 (2021).
50. Rajasree, S. C., Takezawa, Y. & Shionoya, M. Cu(II)-mediated stabilisation of DNA duplexes bearing consecutive ethenoadenine lesions and its application to a metal-responsive DNAzyme. *Chem. Commun.* **59**, 1006–1009 (2023).
51. Torabi, S.-F. et al. In vitro selection of a sodium-specific DNAzyme and its application in intracellular sensing. *Proc. Natl. Acad. Sci. USA* **112**, 5903–5908 (2015).
52. Wang, Z. G., Elbaz, J., Remacle, F., Levine, R. D. & Willner, I. All-DNA finite-state automata with finite memory. *Proc. Natl. Acad. Sci. USA* **107**, 21996–22001 (2010).
53. Wang, Z. G., Elbaz, J. & Willner, I. DNA machines: bipedal walker and stepper. *Nano Lett.* **11**, 304–309 (2011).
54. Thomas, J. M., Yu, H. Z. & Sen, D. A mechano-electronic DNA switch. *J. Am. Chem. Soc.* **134**, 13738–13748 (2012).
55. Lu, C.-H., Cecconello, A., Elbaz, J., Credi, A. & Willner, I. A three-station DNA catenane rotary motor with controlled directionality. *Nano Lett.* **13**, 2303–2308 (2013).
56. Murata, S., Toyota, T., Nomura, S. M., Nakakuki, T. & Kuzuya, A. Molecular cybernetics: challenges toward cellular chemical artificial intelligence. *Adv. Funct. Mater.* **32**, 2201866 (2022).
57. McGhee, C. E., Lake, R. J. & Lu, Y. Preparation of metalloDNAzymes. *Artificial Metalloenzymes and Metallo DNAzymes in Catalysis: From Design to Applications* (eds Diéguez, M. et al.) 41–68 (Wiley-VCH, 2018).
58. Takezawa, Y., Suzuki, A., Nakaya, M., Nishiyama, K. & Shionoya, M. Metal-dependent DNA base pairing of 5-carboxyuracil with itself and all four canonical nucleobases. *J. Am. Chem. Soc.* **142**, 21640–21644 (2020).
59. Mori, K., Takezawa, Y. & Shionoya, M. Metal-dependent base pairing of bifacial iminodiacetic acid-modified uracil bases for switching DNA hybridization partner. *Chem. Sci.* **14**, 1082–1088 (2023).
60. Fujimoto, J., Tran, L. & Sowers, L. C. Synthesis and cleavage of oligodeoxynucleotides containing a 5-hydroxyuracil residue at a defined site. *Chem. Res. Toxicol.* **10**, 1254–1258 (1997).
61. Morningstar, M. L., Kreutzer, D. A. & Essigmann, J. M. Synthesis of oligonucleotides containing two putatively mutagenic DNA lesions: 5-hydroxy-2'-deoxyuridine and 5-hydroxy-2'-deoxycytidine. *Chem. Res. Toxicol.* **10**, 1345–1350 (1997).

Acknowledgements

This work was supported by JSPS KAKENHI Grant Numbers JP18H02081, JP21H02055, JP22K19100 to Y.T., JP21J11325 (Grant-in-Aid for JSPS Fellows) to K.M., and JP21H05022 to M.S. and MEXT KAKENHI Grant Numbers JP21H00384 (Molecular Engine), JP21H05866, JP23H04399 (Molecular Cybernetics) to Y.T., and JP16H06509 (Coordination Asymmetry) to M.S., Japan.

Author contributions

Y.T., K.M., and M.S. conceived and designed the project. K.M., W.-E.H., K.N., and T.X. carried out the experiments with assistance from Y.T. and T.N. Y.T., K.M., and W.-E. H. analyzed the data. Y.T., K.M., and M.S. wrote the manuscript.

Competing interests

The authors declare no competing interests.

Additional information

Supplementary information The online version contains supplementary material available at <https://doi.org/10.1038/s41467-023-40353-3>.

Correspondence and requests for materials should be addressed to Yusuke Takezawa or Mitsuhiro Shionoya.

Peer review information *Nature Communications* thanks Julian Tanner and the other anonymous reviewer(s) for their contribution to the peer review of this work. A peer review file is available.

Reprints and permissions information is available at <http://www.nature.com/reprints>

Publisher's note Springer Nature remains neutral with regard to jurisdictional claims in published maps and institutional affiliations.

Open Access This article is licensed under a Creative Commons Attribution 4.0 International License, which permits use, sharing, adaptation, distribution and reproduction in any medium or format, as long as you give appropriate credit to the original author(s) and the source, provide a link to the Creative Commons licence, and indicate if changes were made. The images or other third party material in this article are included in the article's Creative Commons licence, unless indicated otherwise in a credit line to the material. If material is not included in the article's Creative Commons licence and your intended use is not permitted by statutory regulation or exceeds the permitted use, you will need to obtain permission directly from the copyright holder. To view a copy of this licence, visit <http://creativecommons.org/licenses/by/4.0/>.

© The Author(s) 2023